

# Secondary Coronary Artery Vasospasm Promotes Cardiomyopathy Progression

Matthew T. Wheeler,\* Claudia E. Korcarz,<sup>†</sup>  
Keith A. Collins,<sup>†</sup> Karen A. Lapidos,\*  
Andrew A. Hack,\* Matthew R. Lyons,<sup>†</sup>  
Sara Zarnegar,<sup>†</sup> Judy U. Earley,<sup>†</sup>  
Roberto M. Lang,<sup>†</sup> and Elizabeth M. McNally<sup>†‡</sup>

From the Departments of Molecular Genetics and Cell Biology\*  
and Human Genetics,<sup>‡</sup> and the Department of Medicine,<sup>†</sup> Section  
of Cardiology, University of Chicago, Chicago Illinois

**Genetic defects in the plasma membrane-associated sarcoglycan complex produce cardiomyopathy characterized by focal degeneration. The infarct-like pattern of cardiac degeneration has led to the hypothesis that coronary artery vasospasm underlies cardiomyopathy in this disorder. We evaluated the coronary vasculature of  $\gamma$ -sarcoglycan mutant mice and found microvascular filling defects consistent with arterial vasospasm. However, the vascular smooth muscle sarcoglycan complex was intact in the coronary arteries of  $\gamma$ -sarcoglycan hearts with perturbation of the sarcoglycan complex only within the adjacent myocytes. Thus, in this model, coronary artery vasospasm derives from a vascular smooth muscle-cell extrinsic process. To reduce this secondary vasospasm, we treated  $\gamma$ -sarcoglycan-deficient mice with the calcium channel antagonist verapamil. Verapamil treatment eliminated evidence of vasospasm and ameliorated histological and functional evidence of cardiomyopathic progression. Echocardiography of verapamil-treated,  $\gamma$ -sarcoglycan-null mice showed an improvement in left ventricular fractional shortening ( $44.3 \pm 13.3\%$  treated versus  $37.4 \pm 15.3\%$  untreated), maximal velocity at the aortic outflow tract ( $114.9 \pm 27.9$  cm/second versus  $92.8 \pm 22.7$  cm/second), and cardiac index ( $1.06 \pm 0.30$  ml/minute/g versus  $0.67 \pm 0.16$  ml/minute/g,  $P < 0.05$ ). These data indicate that secondary vasospasm contributes to the development of cardiomyopathy and is an important therapeutic target to limit cardiomyopathy progression. (*Am J Pathol* 2004, 164:1063–1071)**

Cardiomyopathy occurs from mutations in genes encoding the dystrophin glycoprotein complex in both humans and mice.<sup>1–3</sup> In heart and skeletal muscle, genetic mutations destabilize components of the dystrophin glycoprotein complex leading to membrane defects and myocyte loss. Dystrophin is a large cytoskeletal protein that binds

to the transmembrane and cytoskeletal elements of the dystrophin glycoprotein complex.<sup>4</sup> Dystroglycan and sarcoglycan comprise the transmembrane dystrophin glycoprotein complex elements.<sup>5,6</sup> Dystroglycan directly binds the extracellular matrix protein laminin completing the link from the internal cytoskeleton through the membrane to the extracellular matrix.<sup>7</sup> The sarcoglycan complex consists of single transmembrane domain-containing proteins that form a multimeric complex.<sup>6</sup> The sarcoglycan complex serves a mechanosignaling role through its interactions with dystroglycan and filamin-2.<sup>8</sup>

There are six sarcoglycan family members:  $\alpha$ -,  $\beta$ -,  $\gamma$ -,  $\delta$ -,  $\epsilon$ -, and  $\zeta$ -sarcoglycan.<sup>6,9</sup> Mutations in the  $\beta$ -,  $\gamma$ -, and  $\delta$ -sarcoglycan genes produce muscular dystrophy and dilated cardiomyopathy, and mouse models of sarcoglycan mutations recapitulate the human phenotype.<sup>10–13</sup> Cardiomyopathy in the murine models is progressive. By 8 to 10 weeks of age, small foci of degeneration are present and regional uptake of the vital tracer Evans blue dye into cardiomyocytes is distributed randomly and is typically present in 1 to 2% of cardiomyocytes. With time regional fibrosis becomes more evident. Sarcoglycan mutant mice have an increased mortality without evidence of severe edema, consistent with the human clinical course in sarcoglycan deficiency.<sup>14</sup>

The infarct-like pattern of necrosis in  $\beta$ -sarcoglycan or  $\delta$ -sarcoglycan-null mice and in another model of sarcoglycan deficiency, the  $\delta$ -sarcoglycan mutant BIO14.6 cardiomyopathic hamster, suggested that coronary vascular spasm leads to cardiomyopathy progression.<sup>10,15–18</sup> Disruption of the smooth muscle sarcoglycan complex was noted in both  $\delta$ -sarcoglycan and  $\beta$ -sarcoglycan mutant mice<sup>10,11,18</sup> and proposed as a mechanism underlying vasospasm and responsible as a primary etiology of cardiomyopathy. Supporting this, microvascular-filling experiments of coronary arteries demonstrated focal stenoses in  $\beta$ -sarcoglycan and  $\delta$ -sarcoglycan mice consistent with vasospasm. To reduce vasospasm,  $\delta$ -sarcoglycan mutant mice or the BIO14.6 hamster model were treated with the calcium channel antagonist verapamil with reduction of the pathological

Supported by the American Heart Association (grant EI0140075N to E.M.M. and Midwest Affiliate Predoctoral grant 02152362 to M.T.W.), the Muscular Dystrophy Association, the National Institutes of Health (grant HL61322), and the Burroughs Wellcome Fund (to E. M. M.).

Accepted for publication December 11, 2003.

Address reprint requests to Elizabeth M. McNally, M.D., Ph.D., 5841 S. Maryland, MC 6088, Chicago, IL 60637. E-mail: emcnally@medicinebsd.uchicago.edu.

features of cardiomyopathy and microvascular filling defects.<sup>18,19</sup>

$\gamma$ -Sarcoglycan mutant mice lack exon 2 and represent a null allele.<sup>13</sup> Like other sarcoglycan gene mutations, disruption of  $\gamma$ -sarcoglycan destabilizes the entire sarcoglycan complex at the plasma membrane with secondary reduction of the remaining sarcoglycan subunits.<sup>20</sup> Focal degeneration develops in the heart and skeletal muscle of  $\gamma$ -sarcoglycan mutants similar to  $\delta$ - or  $\beta$ -sarcoglycan mutants. We now evaluated the role of smooth muscle sarcoglycan disruption and vasospasm in mice lacking  $\gamma$ -sarcoglycan. Despite an identical pattern of cardiomyopathy to  $\gamma$ -sarcoglycan-null mice, we found no disruption of the vascular smooth muscle sarcoglycan complex in  $\gamma$ -sarcoglycan mutant mice. However, microvascular-filling defects were present in  $\gamma$ -sarcoglycan-null coronary arteries. As there is no intrinsic defect in  $\gamma$ -sarcoglycan-mutant vascular smooth muscle, these findings support a paracrine mechanism whereby degenerating cardiomyocytes produce vascular spasm. Vascular spasm, in this model, may further contribute to cardiomyopathy progression and the development of congestive heart failure. To test whether inhibition of secondary vasospasm limits cardiomyopathy progression, we treated  $\gamma$ -sarcoglycan mutant mice with verapamil and found that verapamil-treated mice had improved cardiac function. These data support that secondary vasospasm arises from primary cardiomyocyte degeneration and identify secondary vasospasm as an important target for therapeutic intervention.

## Materials and Methods

### Animals

Mice lacking  $\gamma$ -sarcoglycan ( $gsg^{-/-}$ ) or  $\delta$ -sarcoglycan ( $dsg^{-/-}$ ) were previously reported.<sup>12,13</sup> Mice were maintained by backcrossing heterozygous null animals into the 129T2/SvEmsJ strain. Animals used in the treatment study were products of a  $gsg^{-/-} \times gsg^{-/-}$  mating after one  $gsg^{+/-}/gsg^{+/-}$  cross and seven generations of crosses between  $gsg^{+/-}$  and normal 129T2/SvEmsJ mice (Jackson Laboratories, Bar Harbor, ME). Animals were housed, treated, and handled in accordance with the guidelines set forth by the University of Chicago's IACUC, the Animal Welfare Act regulations, and the NIH Guide for the Care and Use of Laboratory Animals.

### Immunofluorescence

Heart and quadriceps skeletal muscle were dissected and processed as described.<sup>12</sup> Cryosections of 7 to 10  $\mu$ m thickness were incubated with polyclonal anti- $\gamma$ -sarcoglycan (1:1000),<sup>21</sup> polyclonal anti- $\delta$ -sarcoglycan (1:500),<sup>12</sup> polyclonal anti- $\beta$ -sarcoglycan (1:150),<sup>22</sup> affinity-purified polyclonal anti- $\epsilon$ -sarcoglycan (1:50),<sup>23</sup> affinity-purified polyclonal anti- $\zeta$ -sarcoglycan (1:500),<sup>9</sup> polyclonal anti-dystrophin (1:5000),<sup>24</sup> monoclonal anti-dystrophin (NCL-Dys2, 1:200; Novocastra Laboratories, Newcastle on Tyne, UK), monoclonal anti- $\alpha$ -sarcoglycan (NCL-asarc,

1:100; Novocastra), or monoclonal anti-smooth muscle  $\alpha$ -actin (clone 1A4, 1:1000; Sigma, St. Louis, MO). Secondary goat anti-rabbit or goat anti-mouse Cy3 or fluorescein isothiocyanate-conjugated antibodies (Jackson ImmunoResearch, West Grove, PA) were used. Images were acquired using an AxioScope (Carl Zeiss, Oberkochen, Germany), AxioCam, and Axiovision.

### Preparation of Smooth Muscle Lysates and Immunoblotting

Whole aorta, bladder, and uterus were dissected from strain-matched control mice,  $dsg^{-/-}$  or  $gsg^{-/-}$  and solubilized in lysis buffer [50 mmol/L HEPES, pH 7.5, 150 mmol/L NaCl, 2 mmol/L ethylenediaminetetraacetic acid, 10 mmol/L NaF, 10 mmol/L Na pyrophosphate, 1 mmol/L Na orthovanadate, 10% glycerol, 1% Triton X-100, 50  $\mu$ mol/L phenylmethyl sulfonyl fluoride, plus Complete protease inhibitor (Roche, Mannheim, Germany)]. Heavy microsomes were prepared from normal control mouse skeletal muscle as described.<sup>12,25</sup> Five  $\mu$ g of skeletal muscle microsomes and 50  $\mu$ g of smooth muscle lysate were separated by sodium dodecyl sulfate-polyacrylamide gel electrophoresis. Equal loading was verified by Coomassie staining of duplicate gels. Protein was transferred to Immobilon-P membranes (Millipore, Bedford, MA) and incubated with polyclonal anti- $\delta$ -sarcoglycan (1:5000), polyclonal anti- $\gamma$ -sarcoglycan (1:1000), or anti-smooth muscle actin (clone 1A4, 1:200; Sigma). Goat anti-rabbit or goat anti-mouse horseradish peroxidase-conjugated antibodies were used (1:10,000). Blots were imaged using ECLPLUS (Amersham Pharmacia, Piscataway, NJ) and Biomax MS film (Eastman Kodak, Rochester, NY).

### Vital Staining with Evans Blue Dye

Evans blue dye (20 mg/ml) (Sigma) was dissolved in sterile phosphate-buffered saline. Mice were given intraperitoneal injections at 5  $\mu$ l/g body weight 18 hours before sacrifice.<sup>13</sup> Hearts were excised and frozen for immunofluorescence analysis.

### Verapamil Treatment

Verapamil was administered to mice through dissolution in their drinking water at a concentration of 1 mg/ml.<sup>18,26</sup> Average daily water consumption of 3.5 ml per day provides an average daily dose of 3.5 mg/mouse/day or ~100 mg/kg/day. Steady-state serum concentration using this protocol was approximated at 1  $\mu$ g/ml.<sup>26</sup>  $gsg^{-/-}$  mice ( $n = 10$ ) were treated with oral verapamil starting at 4 weeks of age and treated for 22 weeks.  $gsg^{-/-}$  control mice ( $n = 11$ ) were housed under identical conditions without verapamil. All animals were monitored daily.

### Microvascular Filling

Coronary microvascular perfusion was performed as described.<sup>11,27</sup> Microfil red (1 to 1.5 ml; FlowTech, Carver,

MA) was injected directly into the left ventricular apex. Heart contractions perfused the coronary microvasculature, after which the heart was rapidly excised; fixed in 10% formalin for 24 hours; and cleared by sequential incubations in 25%, 50%, 75%, 95%, and 100% ethanol followed by storage in methyl salicylate. Hearts were scored for the presence or absence of stenosis in coronary vessels, and filled major coronary vessel trees and branches were scored for presence or absence of stenosis. Data collection was performed blinded to treatment group and genotype.

### Echocardiography

All animals in the verapamil treatment study, plus normal, age-matched 129T2/SvEmsJ controls ( $n = 11$ ), underwent echocardiographic study at age 6 months as previously described<sup>28,29</sup> blinded to treatment group and genotype. Anesthesia was induced by administering isoflurane in a closed chamber at 3 to 5% (Ohmeda Fluotec 3; Matrix Medical, Orchard Park, NY) in 80% room air/20% O<sub>2</sub>, followed by 0.5 to 2.0% isoflurane through a nose cone throughout the experiment. A high-frequency 15-MHz linear transducer was used (Sonos 5500; Agilent, Andover, MA) at a frame rate of 120 frames/second. Measurements were performed as described previously.<sup>28,29</sup> Stroke volume was determined from aortic Doppler recordings and two-dimensionally targeted M-mode echocardiographic measurements of the diameter of the proximal ascending aorta during systole from the parasternal long axis view. Stroke volume was calculated from the flow velocity integral of each beat multiplied by the aortic cross-sectional area. Cardiac output was calculated as the product of stroke volume and heart rate. Cardiac index was calculated from cardiac output correcting for animal weight.

### Telemetry

Six animals from each treatment group were monitored for 24 to 72 hours by radio frequency telemetry after implantation of an electrocardiographic radio transmitter (TA10EA-F20; Data Sciences International, St. Paul, MN).<sup>27</sup> Additionally, more than 40 untreated  $gsg^{-/-}$  mice ranging in age from 6 weeks to 1 year of age have similarly been examined with a minimum of 72 hours monitoring.

### Exercise Protocol

$gsg^{-/-}$  mice (ages 3 to 4 months) underwent 10 minutes of exercise by running downhill 10 minutes per day for 3 days at 9 m/minute on a 14 degree incline. After the exercise session on day 3, mice were immediately sacrificed for study.

### Data Analysis

Data are presented as means  $\pm$  SD. Groups were tested for statistical significance using one-way analysis of vari-

ance followed by Student-Newman-Keuls post test (echocardiography); the chi-square test for independence followed by Fisher's exact test (microvascular filling); and Student's unpaired  $t$ -test (heart rate variance). All values given are two-tailed  $P$  values.

### Histopathology Analysis

Heart sections were taken through the short axis from apex to base from the verapamil-treated and untreated groups ( $n = 4$  in each group). Masson Trichrome staining was used to evaluate fibrosis. Sections were scored blinded to genotype and drug treatment status using a scale as follows: 0, no fibrosis; 1, fewer than three areas of fibrosis; 2, greater than three areas of fibrosis; 3, greater than three areas of fibrosis and at least one area greater than 10  $\mu$ m in diameter. Sections were each assigned a score, and the average score from each animal was determined. The mean score from each treatment group was then determined and analyzed using a Student's  $t$ -test. Ten to 65 sections were examined from each animal.

To assess inflammation, three different biotinylated antibodies were used: CD45.2, Ly-6G/Ly-6C, and CD11b/Mac-1. Sections were taken from five different animals in each treatment group. Fifteen fields per animal were examined for the number of immunoreactive cells in each field at  $\times 20$  magnification. The number of cells in each treatment group was averaged and compared.

## Results

### The Coronary Artery Vascular Smooth Muscle Complex Is Intact in $\gamma$ -Sarcoglycan Mutants

$\gamma$ -Sarcoglycan mice develop cardiomyopathy between 12 and 24 weeks of age.<sup>13</sup> To determine how the  $\gamma$ -sarcoglycan-null allele affects expression of the vascular smooth muscle complex, we used antibodies specific to each of the sarcoglycan subunits on sections from cardiac tissue that contained arterial structures. When the vascular smooth muscle layer of coronary arteries from normal mice was examined, we found that  $\beta$ -,  $\delta$ -,  $\epsilon$ -, and  $\zeta$ -sarcoglycan were expressed (Figure 1A). In the adjacent normal cardiomyocytes,  $\gamma$ -sarcoglycan in addition to  $\beta$ -,  $\delta$ -,  $\epsilon$ -, and  $\zeta$ -sarcoglycan were expressed (Figure 1A). An anti-smooth muscle actin antibody was used to confirm the integrity and identity of vascular smooth muscle and to demonstrate that  $\gamma$ -sarcoglycan was not expressed in the arterial smooth muscle (data not shown).

Mutations in a single sarcoglycan subunit produce disruption of the remainder of the sarcoglycan subunits.<sup>12</sup> Consistent with this,  $\delta$ -,  $\beta$ -, and, to a lesser extent,  $\epsilon$ - and  $\zeta$ -sarcoglycan, were reduced in  $gsg^{-/-}$  cardiomyocytes (Figure 1A, adjacent cardiomyocytes). In contrast, the vascular smooth muscle expression pattern did not differ between normal coronary artery vascular smooth muscle and  $\gamma$ -sarcoglycan mutant ( $gsg^{-/-}$ ) coronary vascular smooth muscle.  $\beta$ -Sarcoglycan,  $\delta$ -sarcoglycan,  $\epsilon$ -sarcoglycan, and  $\zeta$ -sarcoglycan were all found at levels

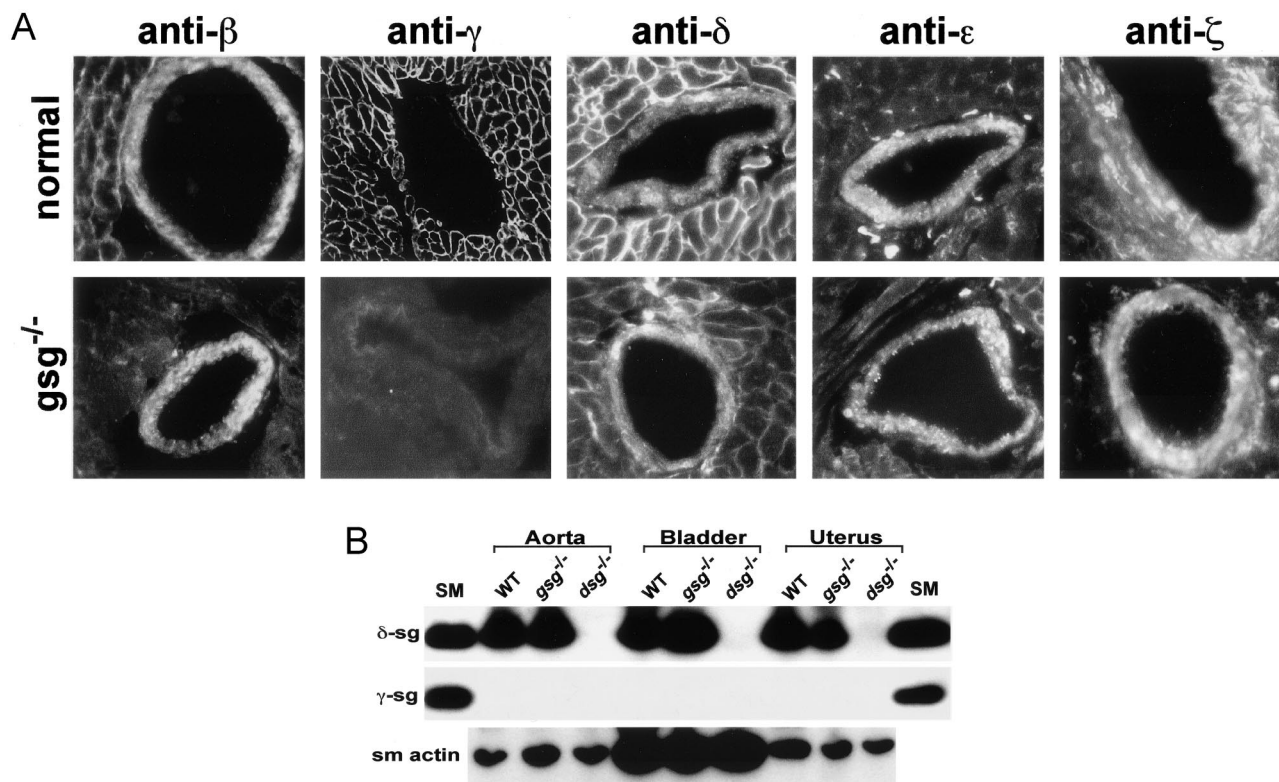


**Figure 1. A:** The coronary vascular smooth muscle sarcoglycan complex. Sections from normal (**top**) or *gsg*<sup>-/-</sup> hearts, including coronary vessels with surrounding cardiomyocytes, were stained with antibodies specific to  $\beta$ -,  $\gamma$ -,  $\delta$ -,  $\epsilon$ -, and  $\zeta$ -sarcoglycan (anti- $\beta$ , anti- $\gamma$ , anti- $\delta$ , anti- $\epsilon$ , and anti- $\zeta$ , respectively). Vascular smooth muscle expresses  $\beta$ -,  $\delta$ -,  $\epsilon$ -, and  $\zeta$ -sarcoglycan in both normal and *gsg*<sup>-/-</sup> hearts. In *gsg*<sup>-/-</sup> hearts, the cardiomyocytes surrounding the coronary vessels have no  $\gamma$ -sarcoglycan and reduced  $\beta$ - and  $\delta$ -sarcoglycan.  $\gamma$ -Sarcoglycan is not present in vascular smooth muscle. **B:** Immunoblots of  $\delta$ -sarcoglycan and  $\gamma$ -sarcoglycan in smooth muscle-containing tissues. Aorta, bladder, and uterus whole protein extracts were made from wild-type (WT), *gsg*<sup>-/-</sup> and *dsg*<sup>-/-</sup> tissues. Skeletal muscle microsomes from wild-type animals (SM) were used as a positive control.  $\gamma$ -Sarcoglycan is striated muscle-specific, and  $\delta$ -sarcoglycan is expressed in *gsg*<sup>-/-</sup> smooth muscle indicating no disruption of the smooth muscle sarcoglycan complex in *gsg*<sup>-/-</sup>. An anti-smooth muscle actin (sm actin) antibody was used to demonstrate loading for the lanes containing smooth muscle-derived lysates (**bottom**).

comparable to that seen in normal coronary smooth muscle.  $\alpha$ -Sarcoglycan was not found in coronary vessels (data not shown).

Using antibodies specific to  $\gamma$ - or  $\delta$ -sarcoglycan, we tested aorta, bladder, and uterus isolated from *gsg*<sup>-/-</sup>, *dsg*<sup>-/-</sup>, and normal mice.  $\gamma$ -Sarcoglycan could not be detected in any of the smooth muscle-containing tissues studied (Figure 1B). Furthermore,  $\gamma$ -sarcoglycan was readily detected in skeletal muscle from control animals.  $\delta$ -Sarcoglycan was detected in *gsg*<sup>-/-</sup> smooth muscle tissues comparable to levels seen in wild-type tissues.  $\delta$ -Sarcoglycan mutants (*dsg*<sup>-/-</sup>), by contrast, show a complete absence of  $\delta$ -sarcoglycan in the smooth muscle tissues, and loss of other smooth muscle sarcoglycans.<sup>11</sup> The smooth muscle sarcoglycan complex is composed of  $\delta$ -,  $\beta$ -,  $\epsilon$ -, and  $\zeta$ -sarcoglycan. In mice mutant for  $\delta$ -sarcoglycan, there is disruption of the vascular smooth muscle sarcoglycan complex whereas in  $\gamma$ -sarcoglycan mutant mice, the vascular smooth muscle sarcoglycan complex remains intact.

### *$\gamma$ -Sarcoglycan-Deficient Animals Show Evidence of Vasospasm*

Microfil microvascular filling was used to examine coronary vessels for the presence of stenoses and dilatations

in *gsg*<sup>-/-</sup>, *dsg*<sup>-/-</sup>, and control animals. This approach was used previously to show that  $\delta$ -sarcoglycan mutant mice and hamsters have coronary artery narrowings as an anatomical indicator of vasospasm.<sup>11,15</sup> Filled coronary vessels were scored for presence or absence of stenoses blinded to genotype. Included in this study are data from *Sur2*<sup>-/-</sup> mice. *Sur2*<sup>-/-</sup> mice develop severe vascular spasm as a consequence of the loss of  $K_{ATP}$  channel activity in vascular smooth muscle.<sup>27</sup> Although the underlying molecular defect differs, *Sur2*<sup>-/-</sup> mice serve as a model of primary vascular smooth muscle spasm. *gsg*<sup>-/-</sup> mice were found to have microvascular filling defects in the coronary vessels (Figure 2) similar in appearance and quality to those seen in *Sur2*<sup>-/-</sup> mice, but at a frequency approximately half that of *Sur2*<sup>-/-</sup> mice (Table 1). The frequency of vascular stenoses in *gsg*<sup>-/-</sup> hearts was equivalent to that seen in *dsg*<sup>-/-</sup> hearts. Normal control mouse hearts were occasionally scored positive for microvascular stenoses but were statistically significantly different from all of *gsg*<sup>-/-</sup>, *dsg*<sup>-/-</sup>, and *Sur2*<sup>-/-</sup> mice (Table 1).

We performed radio frequency electrocardiograph telemetry monitoring on *gsg*<sup>-/-</sup> animals of multiple ages ranging from 6 weeks to 1 year of age, but we found none of the ST elevation that characterizes vasospasm in *Sur2*<sup>-/-</sup> mutant mice (data not shown).<sup>27</sup> Thus, the mech-

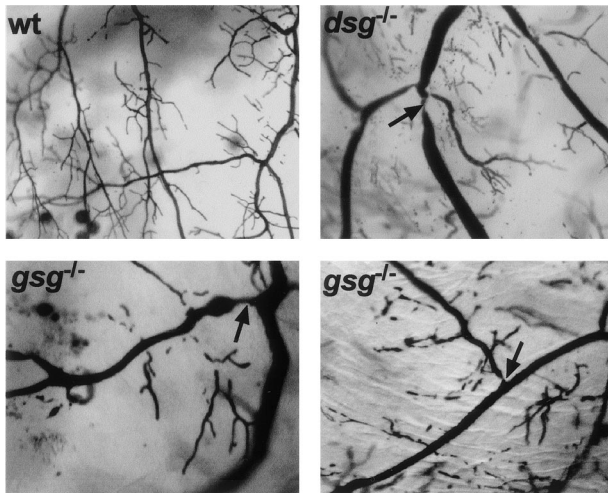


**Figure 2.** Microvascular filling defects in  $\gamma$ -sarcoglycan-null mice. Microfil microvascular filling was used to examine the coronary arterial tree of normal (wt),  $dsg^{-/-}$ , and  $gsg^{-/-}$  hearts. In normal hearts, vascular trees show no evidence of focal narrowing or constriction and generally have smoothly tapered vessels and vessel junctions. In contrast,  $gsg^{-/-}$  and  $dsg^{-/-}$  hearts show evidence of vasospasm with focal narrowings (arrows). Representative images of  $gsg^{-/-}$  microvascular filling typical of the abnormalities seen in both young and old animals (8 and 26 weeks).

anism or severity of vasospasm may differ in these two models of vasospasm. Because  $gsg^{-/-}$  animals do not have disruption of the smooth muscle sarcoglycan complex, vasospasm must occur from a cell extrinsic process.

### Verapamil Treatment Reduces Vasospasm in $gsg^{-/-}$ Hearts

Calcium channel antagonists are frequently used in the treatment of vasospasm. We treated  $gsg^{-/-}$  animals from 4 weeks to 6 months of age with verapamil in their drinking water for an average daily dose of 3.5 mg. Unanesthetized electrocardiograph telemetry did not show significant differences in average heart rate or rhythm between treated and untreated (average heart rate:  $542 \pm 27$  beats per minute verapamil-treated  $gsg^{-/-}$  mice versus  $555 \pm 34$  beats per minute untreated  $gsg^{-/-}$  mice). Abnormal heart rhythms did not differ between treated and untreated animals. Treated mice did show a statistically significant decrease in the variation of heart

**Table 1.** Quantitation of Microfil Microvascular Filling

Genotype	<i>n</i>	% Hearts positive	% Vessels positive	<i>P</i> versus normal
Normal	21	9.5	2.5	n/a
$gsg^{-/-}$	25	36.0	14.3	<0.05
Verap $gsg^{-/-}$	4	0.0	0.0	1
Exercise $gsg^{-/-}$	5	100	28.5	<0.001
$dsg^{-/-}$	19	42.9	12	<0.05
$Sur2^{-/-}$	7	100	22.9	<0.0001

Microfilled hearts were scored for number of major vascular branches filled, and these vessels were scored for evidence of vasospasm (stenosis). Scoring was done blinded to genotype and treatment group. *n* = number of filled hearts scored; Hearts positive, filled hearts scored positive for stenosis; Vessels positive, filled major vascular branches scored positive for stenosis; *P* versus normal, Fisher's Exact test *P* value versus normal.

rate from one 10-second segment to the next versus untreated  $gsg^{-/-}$  mice [ $7.32 \pm 3.29$  beats per minute per 10 seconds (BPM/10s) versus  $16.26 \pm 2.73$  BPM/10s,  $P < 0.0001$ ] consistent with effective verapamil delivery to treated  $gsg^{-/-}$  mice.

Microvascular filling on a limited cohort of the treated  $gsg^{-/-}$  mice and their untreated congenic  $gsg^{-/-}$  controls revealed that verapamil-treated  $gsg^{-/-}$  mice had normal coronary arteries (Table 1). To determine whether exercise exacerbates secondary vascular spasm, a cohort of  $gsg^{-/-}$  mice ( $n = 5$ ) was subjected to 3 days of 10 minutes/day of running downhill. Immediately after the third round of exercise, mice were perfused with Microfil. We found that 100% of exercised  $gsg^{-/-}$  mice had evidence of coronary artery stenoses compared to 36% of unexercised  $gsg^{-/-}$  and 0% of verapamil-treated, unexercised  $gsg^{-/-}$  mice (Table 1). Untreated, unexercised  $gsg^{-/-}$  and  $dsg^{-/-}$  mice had similar frequencies of stenoses. Thus, exercise increased coronary artery vasospasm.

Verapamil treatment reduced histological defects seen in  $gsg^{-/-}$  hearts, including areas of focal necrosis, fibrosis, and inflammation (Figure 3). A blinded scoring system, ranging from 0 to 3, was used to evaluate pathology and revealed average scores of  $0.93 \pm 0.23$  for verapamil-treated  $gsg^{-/-}$  mice and  $1.68 \pm 0.80$  for untreated  $gsg^{-/-}$  mice ( $P = 0.06$ ). The *P* value for this comparison approached, but did not achieve, statistical significance reflecting the regional distribution and variation in focal degeneration that is a pathological hallmark of sarcoglycan-mediated cardiomyopathy. Moreover, this analysis underscores that focal degeneration was still present in verapamil-treated  $gsg^{-/-}$  mice. As shown in Figure 3, areas of fibrosis and inflammation surrounding coronary vessels were also attenuated but not eliminated. We quantified the degree of inflammatory cellular infiltrate using antibodies to leukocytes and macrophages in sections taken from the verapamil-treated and untreated  $gsg^{-/-}$  mice. No significant differences were detected suggesting that the inflammatory cell infiltrate present in  $gsg^{-/-}$  hearts is unaffected by verapamil treatment. Macrophages were equally present in treated versus untreated hearts  $14.3 \pm 10$  versus  $18.0 \pm 18$  cells per field, as were neutrophils,  $11.73 \pm 11.39$  versus  $13.06 \pm 11.20$ , respectively. Additionally, cardiomyocyte plasma membrane defects, as assessed by uptake of Evans blue dye also remained present. Thus verapamil treatment does not eliminate the primary cardiomyocyte degeneration seen in  $gsg^{-/-}$  mice. The degree of improvement produced from verapamil treatment likely reflects the contribution of secondary vasospasm to the progression of cardiomyopathy seen in untreated  $\gamma$ -sarcoglycan-null animals.

### Echocardiography Demonstrates Functional Improvement in Verapamil-Treated $gsg^{-/-}$ Hearts

To examine cardiac function, we performed echocardiography on all untreated  $gsg^{-/-}$  mice, verapamil-treated  $gsg^{-/-}$  mice, and 11 age- and strain-matched normal

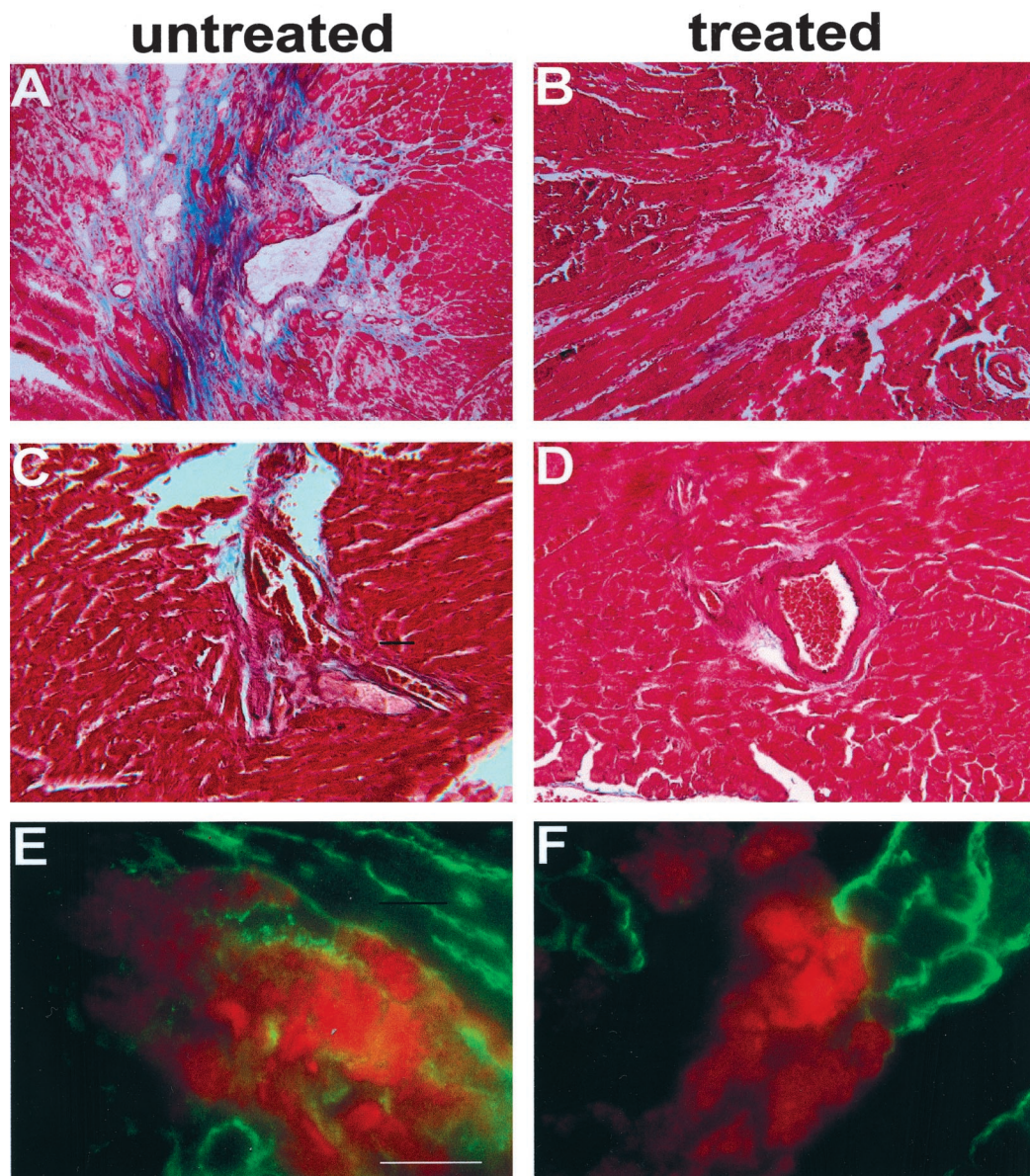


**Figure 3.** Verapamil treatment ameliorates but does not eliminate evidence of cardiomyocyte damage. **A, C, and E:** Representative images of hearts from untreated 26-week-old  $gsg^{-/-}$  mice. **B, D, and F:** Representative images from hearts of  $gsg^{-/-}$  mice treated with oral verapamil for 5 months. **A–D:** Masson trichrome staining of 26-week-old heart sections showing focal necrosis, fibrosis, and inflammatory infiltrate. A reduction in focal necrosis is seen with verapamil treatment. Perivascular inflammation is also reduced with verapamil treatment. **E and F:** Evans blue dye staining (red) shows areas of cardiomyocyte membrane damage. The plasma membranes of cardiomyocytes are stained with anti-dystrophin antibody (green). Scale bar, 10  $\mu$ m.

mice, at age 6 months.  $gsg^{-/-}$  mice were found to have significant functional impairment when compared to normal mice. The calculated cardiac index from Doppler flow at the aortic valve was  $0.68 \pm 0.16$  ml/minute/g untreated  $gsg^{-/-}$  mice versus  $1.55 \pm 0.51$  ml/minute/g normal ( $P < 0.001$ ). Verapamil-treated  $gsg^{-/-}$  mice showed a trend toward improvement in percent fractional shortening ( $44.3 \pm 13.3\%$  treated versus  $37.4 \pm 15.3\%$  untreated). The high variability in fractional shortening reflects the regional cardiac degeneration in  $\gamma$ -sarcoglycan mutant mice. Evidence for hypertrophy was not seen because LV mass was not increased in  $gsg^{-/-}$  compared to control (LV mass index, systole  $3.39 \pm 0.36$  mg/g

untreated  $gsg^{-/-}$  versus  $3.72 \pm 0.40$  mg/g normal; computed by area-length method).<sup>29</sup>

Evidence for frank left ventricular dilation was present only in untreated  $gsg^{-/-}$  mice (3 of 10). In contrast, none of the verapamil-treated  $gsg^{-/-}$  mice were found to have evidence of left ventricular dilation. A younger cohort (age 3 to 4 months) of  $gsg^{-/-}$  mice showed the same distribution (two of five) of dilated cardiomyopathy. Four untreated  $gsg^{-/-}$  mice had shortening fractions under 30%, and had significantly different shortening fractions from normal ( $48.9 \pm 9.6\%$ ) as a group ( $P < 0.05$  versus normal). No verapamil-treated  $gsg^{-/-}$  mice had a fractional shortening below 30%, and as a group, verapamil-

treated *gsg*<sup>-/-</sup> mice were comparable to normal control mice ( $P = 0.28$  treated versus normal) (Figure 4). Hemodynamic data collected by Doppler echocardiography showed that treated *gsg*<sup>-/-</sup> mice developed greater peak velocity at the aortic outflow tract consistent with improved ventricular function with verapamil treatment ( $114.9 \pm 27.9$  cm/second treated versus  $92.8 \pm 22.7$  cm/second untreated,  $P = 0.08$ ). Cardiac indices were significantly improved for treated *gsg*<sup>-/-</sup> mice ( $1.07 \pm 0.30$  ml/minute/g treated versus  $0.68 \pm 0.16$  ml/minute/g untreated,  $P < 0.05$ ), demonstrating that overall, cardiac function was significantly improved with verapamil treatment.

Lastly, we evaluated whether verapamil treatment has an effect on residual expression of the nonmutated sarcoglycans. Mutation of  $\gamma$ -sarcoglycan causes disruption of the remaining sarcoglycans in that they are no longer stable at the plasma membrane (Figure 5).<sup>12,13</sup> We previously showed that mRNA for these remaining sarcoglycans was normal and that protein levels of the remaining, nonmutated sarcoglycan ranged from 10 to 40% of normal levels.<sup>12</sup> Although protein expression can be detected, little to no protein is expressed at the plasma membrane owing to defective assembly and/or instability of the sarcoglycan complex at the plasma membrane. We evaluated whether sarcoglycan expression was qualitatively altered by verapamil treatment, but found that sarcoglycan expression at the plasma membrane remained low to undetectable at the plasma membrane (Figure 5).

### Discussion

Vasospasm has previously been suggested to mediate the progression of cardiomyopathy in sarcoglycan gene mutations and was thought to reflect a primary vascular smooth muscle defect.<sup>11,15</sup> Because  $\gamma$ -sarcoglycan mice have no intrinsic vascular smooth muscle defect, vasospasm is a vascular smooth muscle extrinsic process. We now show that  $\gamma$ -sarcoglycan is not a component of the normal coronary vascular smooth muscle complex and is expressed exclusively in striated muscle. This expression pattern for  $\gamma$ -sarcoglycan is consistent with some previous reports<sup>30-32</sup> but differs from one other.<sup>33</sup> These data are reconciled by the recent identification of the highly related sarcoglycan gene,  $\zeta$ -sarcoglycan.<sup>9</sup>  $\zeta$ -Sarcoglycan shares significant sequence identity with  $\gamma$ -sarcoglycan, so antibodies directed against  $\gamma$ -sarcoglycan may cross-react with  $\zeta$ -sarcoglycan.<sup>9</sup> Furthermore, we now demonstrate, with sarcoglycan-specific antibodies,<sup>9</sup> that  $\gamma$ -sarcoglycan deficiency does not disrupt the expression of the other sarcoglycans in smooth muscle, leaving the normal pattern of vascular smooth muscle sarcoglycan expression intact.

$\gamma$ -Sarcoglycan, like  $\alpha$ -sarcoglycan, is a striated muscle-specific protein. Therefore, the primary defect that produces cardiomyopathy in this model must derive from a defective striated muscle-specific process. It has been suggested that severe skeletal muscle disease can produce cardiomyopathy from compromised respiratory muscle dysfunction.<sup>34</sup> We recently showed that cardio-

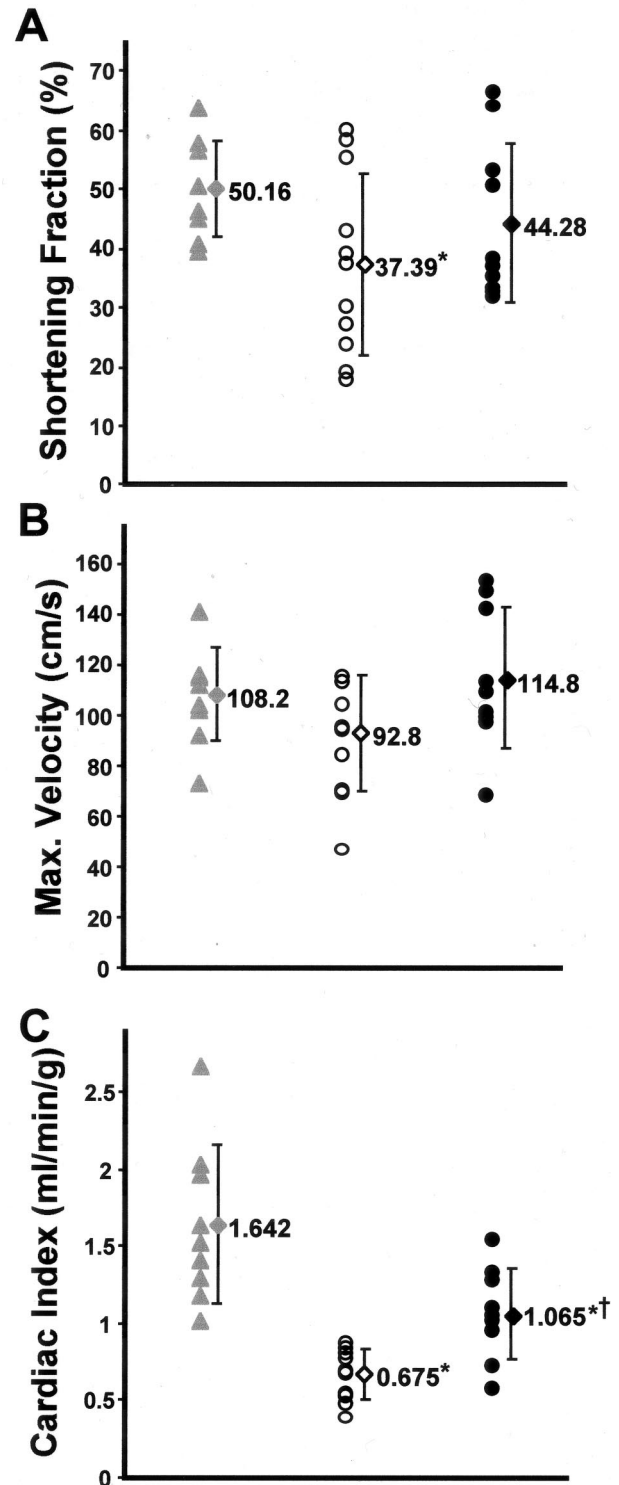


**Figure 4.** Verapamil treatment improves cardiac function. **A–C:** Measurements from echocardiography of 6-month-old normal mice (gray triangles), *gsg*<sup>-/-</sup> mice (open circles), and verapamil-treated *gsg*<sup>-/-</sup> mice (filled circles) are shown. Means  $\pm$  SDs are represented for normal (gray diamond), untreated *gsg*<sup>-/-</sup> (open diamond), and verapamil-treated *gsg*<sup>-/-</sup> (filled diamond) cohorts. Fractional shortening (A), maximal developed velocity at the aortic outflow tract (B), and cardiac index (C) all show functional improvement with verapamil treatment of *gsg*<sup>-/-</sup> mice. \*,  $P < 0.05$  versus normal; †,  $P < 0.05$  versus untreated *gsg*<sup>-/-</sup>.

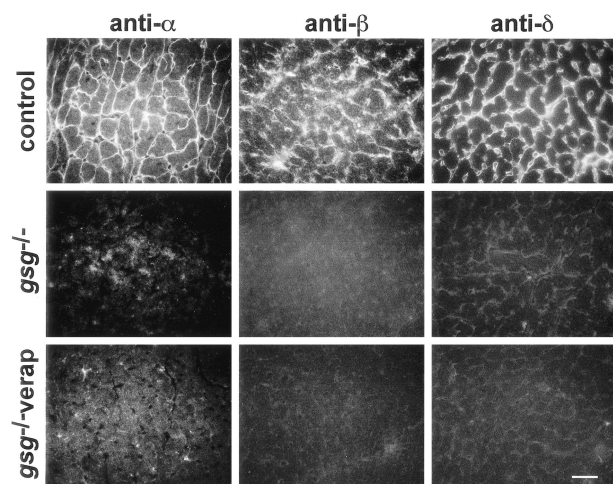


**Figure 5.** Verapamil treatment does not improve expression of the remaining sarcoglycan at the plasma membrane. The major sarcoglycan complex of cardiomyocytes is  $\alpha$ -,  $\beta$ -,  $\gamma$ -, and  $\delta$ -sarcoglycan. Antibodies specific to  $\alpha$ -sarcoglycan,  $\beta$ -sarcoglycan, and  $\delta$ -sarcoglycan were used on normal control and  $\gamma$ -sarcoglycan-null mice ( $gsg^{-/-}$ ) that were treated and untreated with verapamil. Scale bar, 10  $\mu$ m.

myocyte focal necrosis persisted despite transgenic rescue of the skeletal muscle defect in  $\gamma$ -sarcoglycan mutant mice.<sup>35</sup> Therefore, severe skeletal muscle dysfunction is not responsible for the cardiac degeneration in  $\gamma$ -sarcoglycan mutant mice. Interestingly, secondary vasospasm as it occurs in  $\gamma$ -sarcoglycan mutant mice was similar in quality and frequency to that in  $\delta$ -sarcoglycan mice. This suggests that secondary vasospasm may potentially be the major mechanism in  $\delta$ -sarcoglycan gene mutations. Interestingly,  $gsg^{-/-}$  and  $dsg^{-/-}$  mice do not display the same frequency of vasospasm as do  $Sur2^{-/-}$  mice, a model of variant angina with primary vasospasm. Additionally, the temporal pattern of vasospasm in sarcoglycan mutant mice may differ because vascular spasm in this model does not produce characteristic EKG changes seen in both humans and mice with vascular spasm.

Cardiomyopathy in  $gsg^{-/-}$  mice is not hypertrophic, but is variably dilated. Treatment of  $gsg^{-/-}$  mice with verapamil inhibited secondary vasospasm and attenuated cardiomyocyte damage. Cardiomyopathy progression was significantly slowed, but not eliminated, by verapamil treatment of  $gsg^{-/-}$  mice. The degree to which cardiomyopathy progression was slowed reflects the degree to which vasospasm contributes to cardiomyopathy in sarcoglycan deficiency. In these studies, we initiated verapamil treatment early, before the onset of reduced cardiac function and histologically evident cardiomyopathy. We found continued evidence of cardiomyocyte degeneration, seen on histology and vital dye uptake. Cardiomyocyte degeneration remains in  $gsg^{-/-}$  mice treated with verapamil although these degenerative foci appear smaller in area, suggesting that verapamil may aid in protecting cardiomyocytes from damage by their neighboring cells that are undergoing degeneration. It should be noted that the average cardiac index of verapamil-treated  $gsg^{-/-}$  mice was still less than wild-type strain-matched controls. We believe this difference reflects the intrinsic cardiomyocyte defect from sarcogly-

can deficiency. Alternatively, the known negative inotropic action of verapamil may be depressing cardiac function and reducing cardiac output. Additional studies with newer calcium antagonists that lack negative inotropic activity may be more appropriate when considering human trials.

Loss of sarcoglycan complex at the cardiomyocyte membrane leads to cell membrane disruption and membrane permeability defects that are likely to have secondary effects on nearby cardiomyocytes. The observed clustering of Evans blue dye-positive and damaged cardiomyocytes supports a paracrine action that alters nearby cardiomyocytes as well as nearby vascular structures. The mechanism whereby cardiomyocyte damage produces secondary vasospasm may not be limited to this rare form of genetically mediated cardiomyopathy. Indeed, any form of cardiomyocyte damage may lead to secondary vasospasm further propagating the region of cardiomyocyte degeneration. Vasospasm may play a significant role in causing tertiary effects including impairment of function and defects in cardiac conduction. Ultimately, secondary vasospasm may be a significant mechanism for sudden death as well as cardiomyopathy progression.

## References

- Heydemann A, Wheeler MT, McNally EM: Cardiomyopathy in animal models of muscular dystrophy. *Curr Opin Cardiol* 2001, 16:211–217
- Cox GF, Kunkel LM: Dystrophies and heart disease. *Curr Opin Cardiol* 1997, 12:329–343
- Tsubata S, Bowles KR, Vatta M, Zintz C, Titus J, Muhonen L, Bowles NE, Towbin JA: Mutations in the human delta-sarcoglycan gene in familial and sporadic dilated cardiomyopathy. *J Clin Invest* 2000, 106:655–662
- Rafael JA, Brown SC: Dystrophin and utrophin: genetic analyses of their role in skeletal muscle. *Microsc Res Tech* 2000, 48:155–166
- Bonnemann CG, McNally EM, Kunkel LM: Beyond dystrophin: current progress in the muscular dystrophies. *Curr Opin Pediatr* 1996, 8:569–582
- Hack AA, Groh ME, McNally EM: Sarcoglycans in muscular dystrophy. *Microsc Res Tech* 2000, 48:167–180
- Ibraghimov-Beskrovnaya O, Ervasti JM, Leveille CJ, Slaughter CA, Sernett SW, Campbell KP: Primary structure of dystrophin-associated glycoproteins linking dystrophin to the extracellular matrix. *Nature* 1992, 355:696–702
- Thompson TG, Chan YM, Hack AA, Brosius M, Rajala M, Lidov HG, McNally EM, Watkins S, Kunkel LM: Filamin 2 (FLN2): a muscle-specific sarcoglycan interacting protein. *J Cell Biol* 2000, 148:115–126
- Wheeler MT, Zarnegar S, McNally EM: Zeta-sarcoglycan, a novel component of the sarcoglycan complex, is reduced in muscular dystrophy. *Hum Mol Genet* 2002, 11:2147–2154
- Durbeej M, Cohn RD, Hrstka RF, Moore SA, Allamand V, Davidson BL, Williamson RA, Campbell KP: Disruption of the beta-sarcoglycan gene reveals pathogenetic complexity of limb-girdle muscular dystrophy type 2E. *Mol Cell* 2000, 5:141–151
- Coral-Vazquez R, Cohn RD, Moore SA, Hill JA, Weiss RM, Davisson RL, Straub V, Barresi R, Bansal D, Hrstka RF, Williamson R, Campbell KP: Disruption of the sarcoglycan-sarcospan complex in vascular smooth muscle: a novel mechanism for cardiomyopathy and muscular dystrophy. *Cell* 1999, 98:465–474
- Hack AA, Lam MY, Cordier L, Shoturma DI, Ly CT, Hadhazy MA, Hadhazy MR, Sweeney HL, McNally EM: Differential requirement for individual sarcoglycans and dystrophin in the assembly and function of the dystrophin-glycoprotein complex. *J Cell Sci* 2000, 113:2535–2544



13. Hack AA, Ly CT, Jiang F, Clendenin CJ, Sigrist KS, Wollmann RL, McNally EM: Gamma-sarcoglycan deficiency leads to muscle membrane defects and apoptosis independent of dystrophin. *J Cell Biol* 1998, 142:1279–1287
14. Politano L, Nigro V, Passamano L, Petretta V, Comi LI, Papparella S, Nigro G, Rambaldi PF, Raia P, Pini A, Mora M, Giugliano MA, Esposito MG: Evaluation of cardiac and respiratory involvement in sarcoglycanopathies. *Neuromuscul Disord* 2001, 11:178–185
15. Factor SM, Minase T, Cho S, Dominitz R, Sonnenblick EH: Microvascular spasm in the cardiomyopathic Syrian hamster: a preventable cause of focal myocardial necrosis. *Circulation* 1982, 66:342–354
16. Sonnenblick EH, Fein F, Capasso JM, Factor SM: Microvascular spasm as a cause of cardiomyopathies and the calcium-blocking agent verapamil as potential primary therapy. *Am J Cardiol* 1985, 55:179B–184B
17. Factor SM, Sonnenblick EH: Hypothesis: is congestive cardiomyopathy caused by a hyperreactive myocardial microcirculation (microvascular spasm)? *Am J Cardiol* 1982, 50:1149–1152
18. Cohn RD, Durbeej M, Moore SA, Coral-Vazquez R, Prouty S, Campbell KP: Prevention of cardiomyopathy in mouse models lacking the smooth muscle sarcoglycan-sarcospan complex. *J Clin Invest* 2001, 107:R1–R7
19. Factor SM, Cho SH, Scheuer J, Sonnenblick EH, Malhotra A: Prevention of hereditary cardiomyopathy in the Syrian hamster with chronic verapamil therapy. *J Am Coll Cardiol* 1988, 12:1599–1604
20. Hack AA, Cordier L, Shoturma DI, Lam MY, Sweeney HL, McNally EM: Muscle degeneration without mechanical injury in sarcoglycan deficiency. *Proc Natl Acad Sci USA* 1999, 96:10723–10728
21. McNally EM, Duggan D, Gorospe JR, Bonnemann CG, Fanin M, Pegoraro E, Lidov HG, Noguchi S, Ozawa E, Finkel RS, Cruse RP, Angelini C, Kunkel LM, Hoffman EP: Mutations that disrupt the carboxyl-terminus of gamma-sarcoglycan cause muscular dystrophy. *Hum Mol Genet* 1996, 5:1841–1847
22. Bonnemann CG, Passos-Bueno MR, McNally EM, Vainzof M, de Sa Moreira E, Marie SK, Pavanello RC, Noguchi S, Ozawa E, Zatz M, Kunkel LM: Genomic screening for beta-sarcoglycan gene mutations: missense mutations may cause severe limb-girdle muscular dystrophy type 2E (LGMD 2E). *Hum Mol Genet* 1996, 5:1953–1961
23. McNally EM, Ly CT, Kunkel LM: Human epsilon-sarcoglycan is highly related to alpha-sarcoglycan (adhalin), the limb girdle muscular dystrophy 2D gene. *FEBS Lett* 1998, 422:27–32
24. Lidov HG, Byers TJ, Watkins SC, Kunkel LM: Localization of dystrophin to postsynaptic regions of central nervous system cortical neurons. *Nature* 1990, 348:725–728
25. Ohlendieck K, Ervasti JM, Snook JB, Campbell KP: Dystrophin-glycoprotein complex is highly enriched in isolated skeletal muscle sarcolemma. *J Cell Biol* 1991, 112:135–148
26. Morris SA, Weiss LM, Factor S, Bilezikian JP, Tanowitz H, Wittner M: Verapamil ameliorates clinical, pathologic and biochemical manifestations of experimental chagasic cardiomyopathy in mice. *J Am Coll Cardiol* 1989, 14:782–789
27. Chutkow WA, Pu J, Wheeler MT, Wada T, Makielski JC, Burant CF, McNally EM: Episodic coronary artery vasospasm and hypertension develop in the absence of Sur2 K(ATP) channels. *J Clin Invest* 2002, 110:203–208
28. Weiss RE, Korcarz C, Chassande O, Cua K, Sadow P, Koo E, Samarut JRL: Thyroid hormone and cardiac function in mice deficient in thyroid hormone receptor-alpha or -beta: an echocardiograph study. *Am J Physiol* 2002, 283:E428–E435
29. Collins KA, Korcarz CE, Shroff SG, Bednarz JE, Fentzke RC, Lin H, Leiden JM, Lang RM: Accuracy of echocardiographic estimates of left ventricular mass in mice. *Am J Physiol* 2001, 280:H1954–H1962
30. Noguchi S, Wakabayashi-Takai E, Sasaoka T, Ozawa E: Analysis of the spatial, temporal and tissue-specific transcription of gamma-sarcoglycan gene using a transgenic mouse. *FEBS Lett* 2001, 495:77–81
31. Yamamoto H, Mizuno Y, Hayashi K, Nonaka I, Yoshida M, Ozawa E: Expression of dystrophin-associated protein 35DAG (A4) and 50DAG (A2) is confined to striated muscles. *J Biochem (Tokyo)* 1994, 115:162–167
32. Straub V, Ettinger AJ, Durbeej M, Venzke DP, Cutshall S, Sanes JR, Campbell KP: Epsilon-sarcoglycan replaces alpha-sarcoglycan in smooth muscle to form a unique dystrophin-glycoprotein complex. *J Biol Chem* 1999, 274:27989–27996
33. Barresi R, Moore SA, Stolle CA, Mendell JR, Campbell KP: Expression of gamma-sarcoglycan in smooth muscle and its interaction with the smooth muscle sarcoglycan-sarcospan complex. *J Biol Chem* 2000, 275:38554–38560
34. Megency LA, Kablar B, Perry RL, Ying C, May L, Rudnicki MA: Severe cardiomyopathy in mice lacking dystrophin and MyoD. *Proc Natl Acad Sci USA* 1999, 96:220–225
35. Zhu X, Wheeler MT, Hadhazy M, Lam MY, McNally EM: Cardiomyopathy is independent of skeletal muscle disease in muscular dystrophy. *EMBO J* 2002, 16:1096–1098